J. Phys. B: At. Mol. Phys. **15** (1982) 1533–1548. Printed in Great Britain

Elastic scattering of intermediate- and high-energy electrons by N_2 and CO in the two-potential coherent approach

Ashok Jain

Department of Applied Mathematics and Theoretical Physics, Queen's University Belfast, Belfast BT7 1NN, Northern Ireland

Received 23 November 1981, in final form 2 February 1982

Abstract. Elastic differential, integral and momentum transfer cross sections are reported for the scattering of electrons by N_2 and CO in the energy range 40–800 eV. The two-potential approach of Hayashi and Kuchitsu is employed, in which the total interaction potential is represented as a sum of the short- and the long-range potentials. It is found that the interference cross section term arising due to the coherent sum of the scattering amplitudes from the short- and the long-range parts of the interaction potential, is stronger than the pure long-range potential cross section term, of course, in the small angular region ($\leqslant 40°$).

We also study the multiple scattering within the molecule and found that in the multiple scattering series the single–double (SD) term dominates over the pure double–double (DD) term in the whole energy region considered here. However, there is evidence (below 100 eV) that the DD term is compatible with the SD term in the middle angles and exhibits some peaking behaviour at about 90°.

To evaluate elastic scattering amplitudes for each potential, a partial-wave analysis was performed. Results are discussed and compared with the recent absolute measurements. All our results are in very good accord with the observed data.

1. Introduction

The scattering of electrons by molecules at intermediate energies is a most difficult and challenging job. The existing techniques for studying low-energy electron scattering with molecules (see, for example, a recent review by Lane 1980) are prohibitively difficult for higher energies, since more and more electronic states become energetically accessible (for the definition of low, intermediate and high energies, in the present context, see the review article by Truhlar *et al* 1979). As the energy increases, rotational, vibrational and then electronic channels become active and consequently an exact treatment of the process becomes almost impossible. However, under certain circumstances, the Born–Oppenheimer approximation is valid and the use of a fixed-nuclei approximation allows one to obtain an infinite set of coupled integro-differential equations. This set can be truncated to a finite number and solved numerically. The use of these so called close-coupling methods is limited (due to present computers) to roughly about ionisation thresholds (10–15 eV). On the other hand, the techniques of high-energy electron scattering (where the interaction is not very strong) such as the Born, the polarised Born, the Glauber approximations, etc, can be extended to

0022-3700/82/101533+16$02.00

the intermediate-energy region by incorporating higher-order terms in the Born series or by carefully taking into account the distortions of the incident plane wave, exchange and the correct polarisation of the target. Unfortunately, these extensions fail at a certain energy boundary and the subsequent progress at intermediate energy becomes more and more tedious. Truhlar *et al* (1979) have developed extensively an effective potential approach which works quite well up to an energy of 50 eV. They have done a great deal of work on the elastic and inelastic scattering of electrons with H_2, N_2, CO and CO_2. However, beyond 50 eV, their methodology again seems to be very difficult. However, the intermediate-energy region, even the upper end of it, is very important for electron impact spectroscopy. Knowledge of intermediate-energy electron cross sections is required in modelling the different laser, cometary and interstellar plasmas. In this paper, our aim is to present some reliable theoretical data for the elastic differential, integral and momentum transfer cross sections for the electron scattering by N_2 and CO in the energy region 40–800 eV. These molecules constitute a part of our atmosphere and their cross sections are needed in many scientific disciplines. In addition, we also investigate the multiple scattering within the molecule at all energies considered here. In the following paragraphs we discuss the salient features of the present calculations.

A simple approach for e–molecule elastic scattering at intermediate and high energies is to treat the individual atoms in the molecule as independent scattering centres so that the amplitude for scattering by the molecule can be obtained by adding the amplitudes for scattering by the individual atoms with proper allowance for phase differences. The resulting cross section, after averaging over all molecular orientations, is the so called independent-atom model (IAM) and has been used a long time quite successfully at high impact energies. The first calculation using the IAM for the intermediate-energy region was carried out by Bullard and Massey (1931) for e–N_2; they considered the range 30–780 eV. Later, Truhlar (1972) discussed this IAM methodology, introduced by Massey (1935) in the context of e–N_2 elastic scattering. The concept of independent scattering centres becomes invalid when the wavelength of the incoming electron is comparable with the atomic separation in the molecule. Therefore, the IAM is a possible simple method that can be applied to electron–molecule scattering at intermediate and high energies. In the past, several calculations using the IAM were carried out for e–N_2, e–O_2 (Wedde and Strand 1974 and references therein) and e–CO (Khare and Raj 1979) from 1 keV to below 50 eV in the former case and at 400 eV in the latter case. In fact, the success of these IAM cross sections depends upon the accuracy of the atomic scattering amplitudes. Since the IAM cross sections agree qualitatively (quantitatively, these numbers sometimes differ from experiment by a factor of two) and reproduce the angular dependence of the measurements, it appears reasonable to employ the IAM for further studies. Such studies should incorporate some or all of the following factors: (i) multiple scattering within the molecule, (ii) anisotropic terms in the static potential (these terms are inherent in an actual e–molecule scattering problem; at very low energies, such terms decide the mode of the collision), (iii) an induced polarisation (spherical and non-spherical) potential including non-adiabatic effects in the (apparent) polarisability of the molecule (if the incident electron energy is above 100 eV, a non-adiabatic polarisation potential must be used), (iv) valence–core effects due to the formation of chemical bonds in the molecule, (v) exchange effects and (vi) the effects of molecular rotation and vibration (however, such effects are negligible if the collision time is very small compared with the vibrational or rotational periods).

In practice, it is not possible to take into account all the above factors even for the simplest problem of e–H_2. However, we would like to emphasise that by including the above factors in the IAM framework, our aim is to make the physics in this energy range more transparent, in addition to comparing the calculations with the observed data.

Hayashi and Kuchitsu (1976a) gave a two-potential formalism to describe the electron scattering with molecules at intermediate and high energies. They represent the interaction energy between the electron and the target molecule by a sum of a short-range potential V_S and a long-range potential V_L. In the zeroth-order approximation, V_S can be written as the sum of spherical potentials located at each atom of the molecule; then their method is equivalent to the IAM method. V_L is the sum of both the permanent and the induced long-range potentials and has a one-centre nature since at large distances, the electron sees the molecule as a point dipole or quadrupole. The aproach of Hayashi and Kuchitsu should yield good results since it includes the long-range effects coherently (in contrast to the recent two-potential approaches (Choi *et al* 1979, Lee and Freitas 1981) which add the long-range parts of the cross section incoherently) and allows multiple scattering within the molecule. Another advantage of this theory is that it can be extended in a straightforward manner for rotationally and/or vibrationally inelastic collisions at intermediate energies. A full application of Hayashi and Kuchitsu's approach has never been made for either system studied in the present paper. Hayashi and Kuchitsu (1976b) first applied their method to e–N_2, for which they neglected V_L and studied the effect of multiple scattering in the energy region 100–500 eV. They found that the single–double (SD) term in the multiple scattering series reduced the IAM cross sections by a considerable amount. Their other study was for H_2 (Hayashi and Kuchitsu 1977), for which they considered both V_L and V_S but neglected multiple scattering (this approximation is allowed for H_2 because H is a weak scattering centre and therefore multiple scattering effects should be small). It is clear from their results for e–H_2 that the contributions coming from V_L and V_S separately should be treated in a coherent manner.

We therefore think it extremely important and interesting to use Hayashi and Kuchitsu's methodology in more detail and test its physics for isoelectronic systems like N_2 and CO. Since the cross sections of N_2 and CO are similar to each other at intermediate and high energies (actually they are similar at lower energies too, see, for example, Onda and Truhlar 1980, Truhlar *et al* 1972a), it would be interesting to see how the multiple scattering differs in the two systems. Although we neglect exchange and the non-spherical part of the long-range potential, the errors due to the latter effects should not be serious in the energy range (40–800 eV) considered here. However, below 100 eV, the present calculations require a proper account of exchange and of the anisotropic part of the short-range potential. Since we use the zeroth-order version of the two-potential approach of Hayashi and Kuchitsu, we call this approximation the modified independent-atom model (MIAM). Next we give a brief account of the other theoretical and experimental activities on elastic scattering by N_2 and CO during the last decade.

A summary of the elastic scattering of electrons from N_2 has been given very recently by Shyn and Carignan (1980). We shall not repeat the details here, but would like to add a few more theoretical studies on e–N_2, not included in the table of Shyn and Carignan. The first is due to Hayashi and Kuchitsu (1976b) discussed earlier and the other is made by Choi *et al* (1979). Choi *et al* call their method a two-potential approach, but eventually their cross sections depend upon the atomic scattering

amplitudes (we feel that all such methods which employ atomic scattering amplitudes should be referred to as modified IAM methods). Dalba *et al* (1980) have measured absolute total (elastic and inelastic) cross sections for N_2, O_2 and NO. It is clear from Shyn and Carignan's table that the theoretical work lags well behind the experiments at all energies. In contrast, the work on CO at intermediate and high energies, has not made much headway. Bromberg (1970) and Dubois and Rudd (1976) made absolute measurements for e–CO above and at 200 eV. Except for the very-low-energy ($\leqslant$30 eV) measurements (with which we are not concerned here) the only experimental results at intermediate energies are the normalised absolute measurements of Truhlar *et al* (1972a) at 20 eV and the relative measurements of Truhlar *et al* (1972b) in the range 6–80 eV over the angular range 15–85°. More recently, absolute values of differential, integral and momentum transfer cross sections have been determined by Tanaka *et al* (1978) at 3–100 eV for the angular range 15–135°. For pure vibrational excitation, Chutjian and Tanaka (1980) have measured normalised absolute DCS at electron energies of 3 to 100 eV. Theoretically, the only calculations are due to Khare and Raj (1979) at 400 eV and by R T Poe and co-workers (see the reference 16 in the paper by Tanaka *et al* 1978) in the range 50–500 eV. The calculation of Khare and Raj (1979) used the IAM and included the long-range effects for each atom separately, which seems to be inconsistent because at large distances the electron sees the molecule as a whole. It is therefore clear that in order to explore the observed data for e–N_2 and e–CO collisions in the present energy region, more theoretical work is required. Multiple scattering within a heteronuclear molecule has never been investigated before. Yates and Temney (1972) have also studied multiple scattering in the Glauber approximation for N_2.

In the following section, we give relevant formulae and in the next section results are discussed. Conclusions are presented in § 4.

2. Theory

2.1. Cross section formulae

We represent the interaction potential between the incoming electron and the target molecule as

$$V(r) = V_S(r) + V_L(r) \tag{1}$$

where

$$V_S(r) = \sum_{i=1}^{N} V_i(|\boldsymbol{r} - \boldsymbol{R}_i|) \tag{2}$$

is the short-range potential and V_L is the long-range part of the potential. In equation (2) $V_i(r)$ is the spherical potential located at the ith atom, N is the number of atoms in the molecule, and $\boldsymbol{r}$ and $\boldsymbol{R}_i$ are, respectively, the position vectors of the incoming electron and the ith atom of the molecule. The $\boldsymbol{r}$ and $\boldsymbol{R}_i$ are measured from the centre of mass of the molecule.

Formulae for the differential cross section and the multiple scattering series have been obtained by Hayashi and Kuchitsu (1976a). We shall not repeat all of this analysis and give only the formulae relevant to the present calculations. Assuming

V_L to be local and spherically symmetric, the differential cross section is written as

$$\frac{d\sigma}{d\Omega} = |f_L|^2 + 2|f_L| \sum_{i=1}^{N} |f_i| \cos(\eta_L - \eta_i) \frac{\sin qR_i}{qR_i} + I_S + I_{SS} + I_{SD} + I_{DD} \tag{3}$$

where f_L and f_i are the scattering amplitudes due to V_L and V_i, respectively, q is the momentum transfer ($q = 2k \sin \theta/2$, where k is the wavenumber of incident electron), and

$$I_S = \sum_{i=1}^{N} |f_i|^2 \tag{4}$$

$$I_{SS} = \sum_{i \neq j}^{N} f_i^* f_j \sin(qR_{ij})/qR_{ij} \tag{5}$$

$$I_{SD} = \frac{i}{k} \sum_{i \neq j}^{N} (f_i + f_j)^* \sum_{l_1 l_2 l_3} (2l_1+1)(2l_2+1)(2l_3+1) \times \begin{pmatrix} l_1 & l_2 & l_3 \\ 0 & 0 & 0 \end{pmatrix}^2 P_{l_2}(\cos\theta) j_{l_3}^2(kR_{ij}) A_{l_1}(k, j) A_{l_2}(k, i) \tag{6}$$

$$I_{DD} = \frac{\pi}{k^2} \sum_{i \neq j}^{N} \sum_{l_3} (2l_3+1) j_{l_3}^2(kR_{ij}) \sum_{m_3} \left| \sum_{l_1 l_2} (2l_1+1)(2l_2+1)^{1/2} \begin{pmatrix} l_1 & l_2 & l_3 \\ 0 & 0 & 0 \end{pmatrix} \times \begin{pmatrix} l_1 & l_2 & l_3 \\ 0 & -m_3 & m_3 \end{pmatrix} Y_{l_2, -m_3}(\theta, 0) A_{l_1}(k, j) A_{l_2}(k, i) \right|^2 . \tag{7}$$

In equations (4)–(7), θ is the scattering angle, R_{ij} is the distance between the ith and jth atoms of the molecule, $j_n(x)$ is a spherical Bessel function of order n, $P_l(x)$ is a Legendre polynomial, $Y_{l,m}(\theta, \phi)$ is a spherical harmonic,

$$\begin{pmatrix} l_1 & l_2 & l_3 \\ m_1 & m_2 & m_3 \end{pmatrix}$$

are the 3-j symbols and the quantity $A_l(k, i)$ is defined as

$$A_l(k, i) = \exp(i\delta_l^{(i)}) \sin \delta_l^{(i)} \tag{8}$$

where $\delta_l^{(i)}$ is the phaseshift due to the ith atom. In equation (3), η is defined by

$$f = |f| \exp(i\eta). \tag{9}$$

In the definition of our differential cross section (equation (3)), we have neglected double and triple scattering by V_L and V_S. Also, in the multiple scattering terms (I_{SS}, I_{SD} and I_{DD}), we do not include off-the-energy-shell matrix elements (NFES, see the original text of Hayashi and Kuchitsu 1976a). For V_i, the Yukawa-type potential

$$V_i(r) = -\frac{Z_i}{r} \sum_m \gamma_m \exp(-\lambda_m r) \tag{10}$$

with atomic number Z_i is used. The coefficients γ_m and λ_m are taken from Cox and Bonham (1967). The atomic scattering amplitude is obtained from a sum of partial waves

$$f(\theta) = (2ik)^{-1} \sum_{l=0}^{\infty} (2l+1)[\exp(2i\delta_l) - 1] P_l(\cos\theta). \tag{11}$$

The phaseshifts δ_l were calculated using a modified version of a computer program originally written by Yates (1971), and $f(\theta)$ was computed with a high degree of accuracy by retaining up to 100 partial waves for energies as high as 800 eV. However, below 100 eV, only about 30 partial waves were sufficient to yield converged cross sections.

2.2 Polarisation potential

For incident energies below 100 eV, we used an adiabatic polarisation potential for both CO and N_2 (Truhlar and Van-Catledge 1978, Onda and Truhlar 1979, 1980, Rumble and Truhlar 1979). It is given by

$$\begin{aligned} V_L(r) &= V_0^p(r_1) && r \leqslant r_1 \\ &= V_0^p(r_2) && r_1 < r \leqslant r_2 \\ &= -\frac{\alpha_0}{2r^4} - \frac{D_0^p}{r^6} && r_2 < r \end{aligned} \tag{12}$$

where the various parameters in equation (12) are given in table 1 for both the molecules at the equilibrium internuclear distance (R_e). Above 75 eV, we employ the following polarisation potential

$$V_L(r) = \frac{-\alpha_0}{2r^4}[1 - \exp(-r/r_c)^5]. \tag{13}$$

Table 1. Parameters (in au) for polarisation potentials for N_2 and CO (for references, see the text) (equation (12)).

Parameter	N_2	CO
R_e	2.068	2.136
α_0	11.55	13.34
r_1	2.70	2.74
r_2	1.35	1.15
D_0^p	2.818	2.54
$V_0^p(r_1)$	−0.116	−0.175
$V_0^p(r_2)$	−0.05	−0.07

In equation (13), α_0 is the polarisability to be taken constant at R_e and r_c is the cut-off parameter which is definite and defined (in the units of the Bohr radius a_0) as (Choi *et al* 1979)

$$r_c = \tfrac{1}{2}R_e + 1\ a_0 \tag{14}$$

However, above 100 eV, we do not use a constant value of α_0 as defined in equation (13). Instead, we make use of apparent polarisabilities different for different energies, as given, for example for N_2, by Jansen *et al* (1976).

3. Results and discussion

To evaluate f_L and f_i due to V_L and V_i respectively, we performed partial-wave analyses. For f_i we could evaluate phaseshifts with high accuracy ($\sim 10^{-4}$) but the

same criterion of accuracy could not be maintained for the evaluation of f_L. Here, we include phaseshifts (greater than 100) only up to an accuracy of 10^{-3}. No attempt was made to check the results for various cut-off values (r_c).

Figures 1 and 2 show the contributions of I_{SD} (equation (6)) and I_{DD} (equation (7)) (relative to I_S, equation (4)) for N_2 and CO, respectively, at 50, 60, 100 and 500 eV. Summation over l_1, l_2 and l_3 in equations (6) and (7) converged well with about 14 partial waves. The multiple scattering within these isoelectronic molecules almost agrees in shape. At 50 eV, the maximum contribution of I_{SD} for N_2 and CO occurs at 80 and 60° respectively, while at 60 eV the same contribution occurs at 75 and 55° respectively. At higher energies, for example at 100 eV, I_{SD} contributes most around 20° for each molecule. This means that as the energy increases,

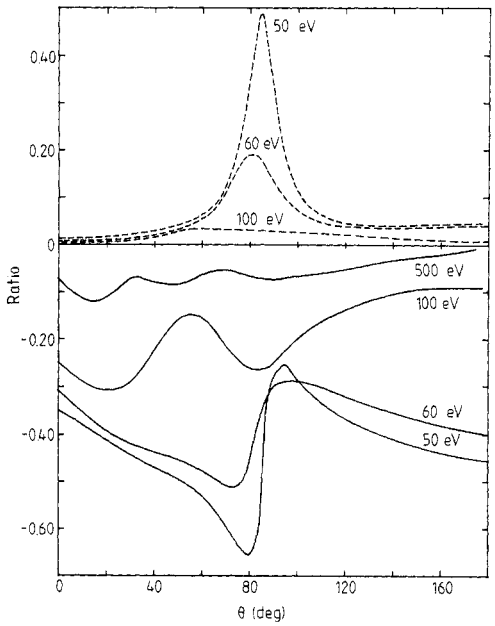

Figure 1. Contribution of single–double (I_{SD}) and double–double (I_{DD}) terms (relative to I_S, equation (3)) at various energies for e–N_2: full curves, I_{SD} (NFES) and broken curves, I_{DD} (NFES).

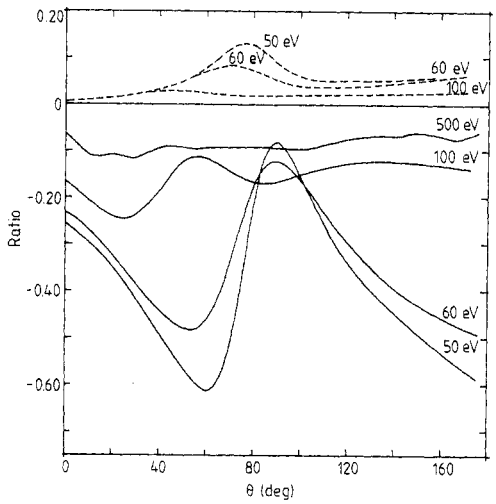

Figure 2. Same caption as for figure 1, but for CO.

multiple scattering is significant in the forward direction. Quantitatively, multiple scattering within N_2 is stronger than within CO. Both the figures show a peak ($\leq$60 eV) in I_{DD} at about 80°, with the difference that the N_2 peak is sharp and has a larger amplitude. As the energy increases, the contributions from I_{SD} and I_{DD} decrease. About 200 eV, I_{DD} is negligible but I_{SD} still reduces the IAM cross sections by at least about 10%. About 500 eV, I_{SD} still contributes very little and at 800 eV this contribution reduces to about 4%. Figure 3 displays separately the contribution to the differential cross section due to V_S, V_L and the interference between V_S and V_L (we call it V_{SL}). It is clear that the V_{SL} term is strong enough to make a significant contribution in the forward angular region. At about 800 eV, contributions due to V_L and V_{SL} are appreciable only below 10°, while at lower energies, for example, at 40 eV, V_{SL} contributes up to 30°. At 100 eV, we also show the same contribution in the e–CO case.

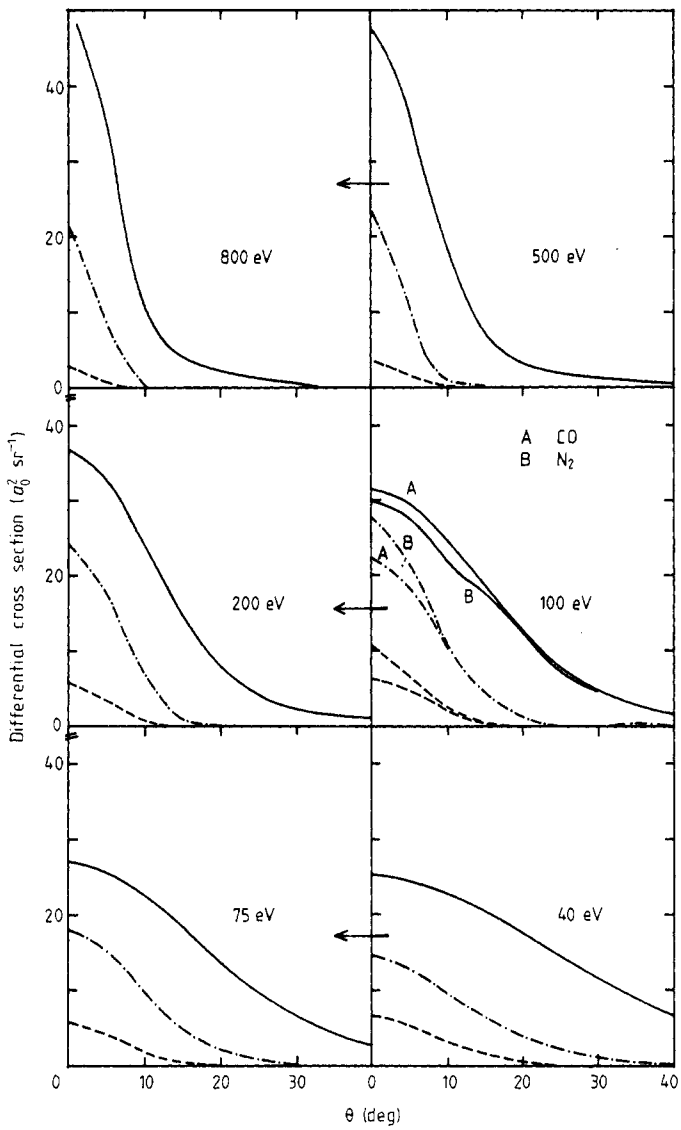

Figure 3. Contribution of V_S, V_L and V_{SL} to the differential cross sections for e–N_2 and e–CO (for 100 eV only). Full curves, V_S; broken curves, V_L and chain curves, V_{SL}. An arrow indicates the scale to be followed.

In figures 4–7 we present the results of our calculation on the differential cross sections for N_2 in the range 40–800 eV. Figure 4 and 5 also show the DCS for CO (broken curves) at 40, 50, 60, 75 and 100 eV, just to make a direct comparison of differential cross sections for both the isoelectronic molecules. In figure 4, the results for N_2 (full curves) are compared with recent measurements of Shyn and Carignan (1980), Dubois and Rudd (1976) and Srivastava *et al* (1976). The agreement between theory and experiment is good except at the intermediate angles (70–110°), where the theoretical dip is deeper, although it occurs near the same angle. It is to be noted that in this angular range I_{SD} also has a peak to soften this dip but, due to a corresponding peak in I_{DD}, the multiple scattering could not soften it. Thus, it is

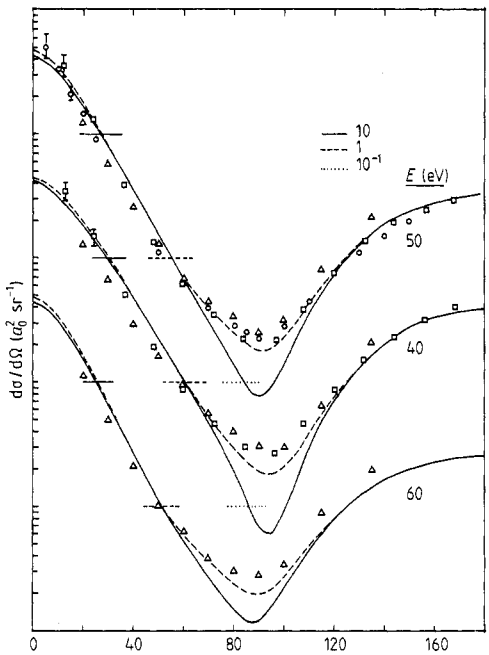

Figure 4. Elastic DCS for e–N_2 and e–CO collisions. Present theory (equation (2)). Full curves, N_2 and broken curves, CO. The experimental data are from: ●, Bromberg (1970); ○, Dubois and Rudd (1976); △, Srivastava *et al* (1976); □, Shyn and Carignan (1980) and ×, Herman *et al* (1976).

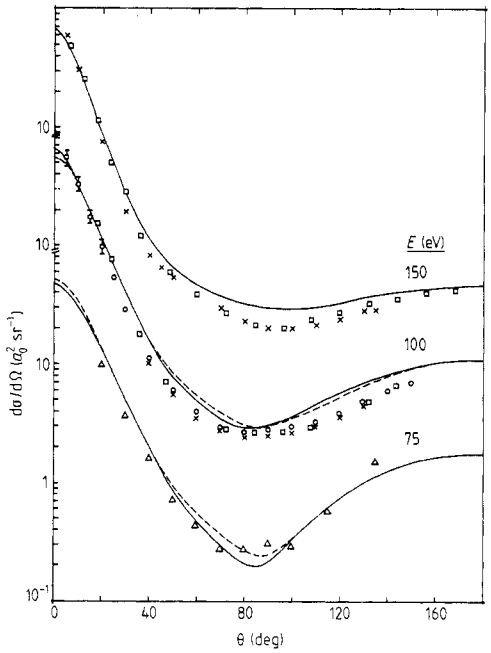

Figure 5. Same caption as for figure 4.

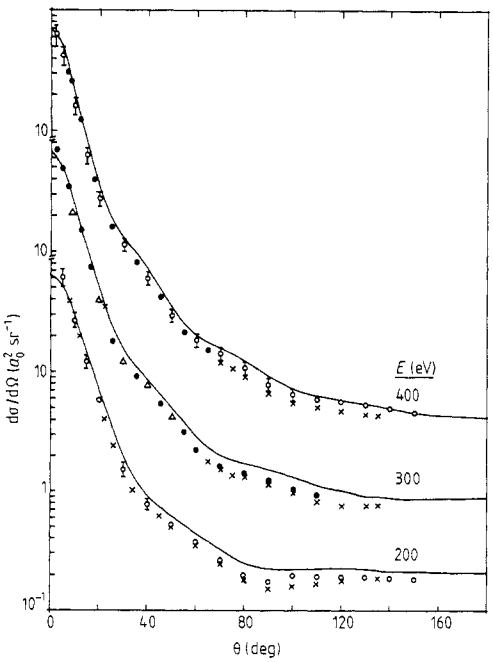

Figure 6. Same caption as for figure 4.

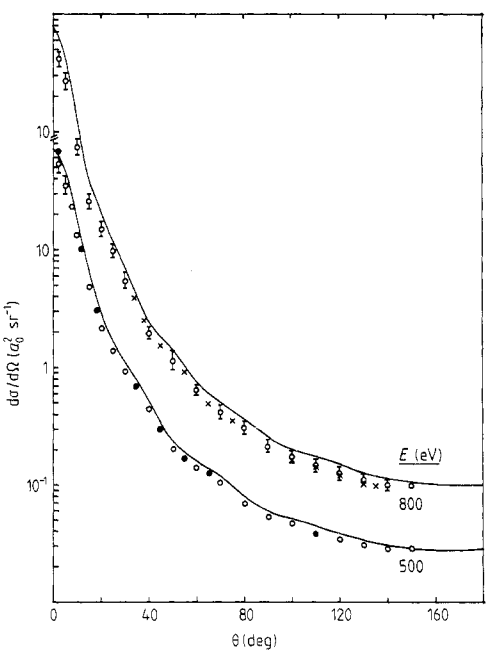

Figure 7. Same caption as for figure 4.

expected that the anisotropy of the true shielded potential would considerably improve results in this angular part (see also the discussion by Choi *et al* 1979). At 75 and 100 eV (figure 5) again, the agreement is reasonably good at all angles. At 150 eV (figure 5), the present curve is about 35% higher than the experiment in the range 70–110° and about 30% beyond 110° at 100 eV. This discrepancy at intermediate and higher angles ($\theta \geq 110°$) is not found at energies greater than 200 eV. Figures 6 and 7 further show the present calculations for N_2 at 200–400 and 500–800 eV respectively. In this energy range, theory predicts very good results in accord with the absolute measurements of Bromberg (1970) and Dubois and Rudd (1976). At small angles the present cross sections are better than the other calculations reported so far (Hayashi and Kuchitsu 1976b, Choi *et al* 1979). This proves our earlier claim that, in any two-potential formalism, a coherent sum of the two contributions should be employed.

Comparison with other theoretical calculations will now be made for N_2 at 50 eV. For vibrationally–electronically elastic (rotationally summed) e–N_2 scattering, Onda and Truhlar (1979) performed calculations including static, exchange and polarisation interactions calculated by the INDOX/1s method and the semiclassical exchange approximation with abiabatic polarisation. A comparison between their results and our result is shown in table 2, along with the absolute measurements of Srivastava *et al* (1976) and Dubois and Rudd (1976). Also shown in this table are the IAM (employing a phenomenological, multiparameter potential, expanded from a single centre in multipoles and including polarisation also) calculations of Sawada *et al* (1974). The results of the latter authors are in very poor agreement with experiment at almost all angles when compared with the calculations of Onda and Truhlar and

Table 2. The DCS for e–N_2 at 50 eV (in units of a_0^2 sr^{-1}). Numbers in parentheses are powers of ten that multiply the corresponding values of the cross section.

	Theory			Experiment	
θ (deg)	Sawada *et al* (1974)	Onda and Truhlar (1979)	Present	Srivastava *et al* (1976)	Dubois and Rudd (1976)
0	2.7 (1)	5.61 (1)	4.16 (1)	—	—
5	2.5 (1)	4.39 (1)	3.83 (1)	—	5.14 (1)
10	2.1 (1)	3.14 (1)	3.08 (1)	—	3.32 (1)
15	1.6 (1)	2.19 (1)	2.28 (1)	—	2.14 (1)
20	—	1.50 (1)	1.64 (1)	1.52 (1)	1.40 (1)
25	—	1.02 (1)	1.15 (1)	—	8.93
30	7.0	6.89	7.73	5.79	5.68
40	—	3.27	3.40	2.34	2.47
50	—	1.64	1.55	1.06	1.14
60	1.35	8.66 (−1)	6.79 (−1)	6.47 (−1)	6.32 (−1)
70	—	5.39 (−1)	3.21 (−1)	4.19 (−1)	4.07 (−1)
80	—	4.37 (−1)	1.42 (−1)	2.98 (−1)	2.89 (−1)
90	6.8 (−1)	4.26 (−1)	7.57 (−2)	2.24 (−1)	2.36 (−1)
100	—	5.29 (−1)	1.41 (−1)	2.85 (−1)	2.84 (−1)
110	—	7.85 (−1)	3.72 (−1)	—	4.63 (−1)
120	8.2 (−1)	1.19	7.68 (−1)	—	7.48 (−1)
130	—	1.67	1.28	—	1.12
140	—	2.17	1.84	—	1.50
150	1.30	2.66	2.37	—	1.90

the present author. At large angles ($\geq 100°$) our results are better than the results of Onda and Truhlar and at smaller angles both these latter calculations are almost equally good. The greatest discrepancy between the present results with theory and experiment occurs at 90°, where our result is smaller by a factor of three, while the result of Onda and Truhlar is greater by a factor of two. Onda and Truhlar's theory produces too shallow a dip at intermediate angles while the present theory gives a dip deeper than the observed one.

For CO, our cross sections for energies 40–800 eV are plotted in figures 8–10. In figures 8 and 9, which are for energies at and below 100 eV, we compare the present theoretical differential cross sections with the experimental data of Tanaka *et al* (1978) and of Truhlar *et al* (1972b). Also shown in these figures are the theoretical calculations

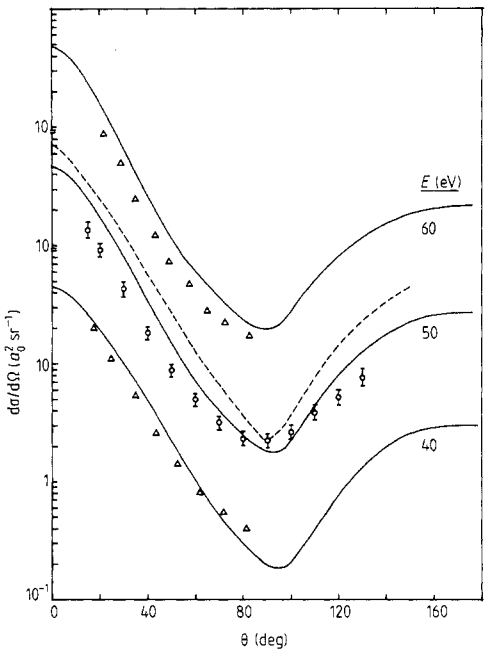

Figure 8. Elastic DCS for e–CO collisions. Present theory, full curve; calculations of Choi *et al* (1979), broken curve. Experimental values: ○, Tanaka *et al* (1978); △, Truhlar *et al* (1972b).

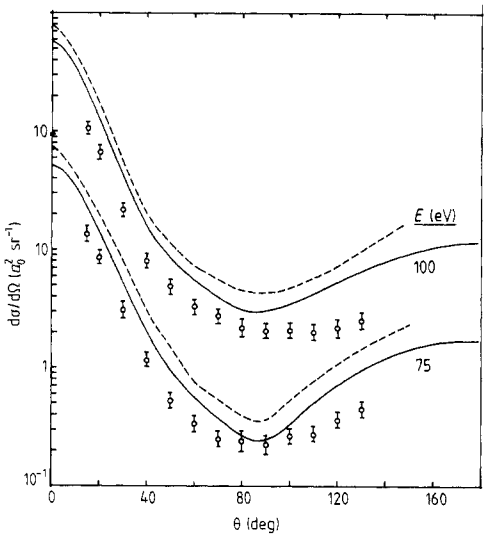

Figure 9. Same caption as for figure 8.

of e–CO elastic cross sections by Choi *et al* (1979) (see, also reference 16 in the paper of Tanaka *et al* 1978). It can be seen from these figures that, within the experimental error, the present theoretical curves are in qualitative agreement with both the laboratory measurements. On the other hand, the theoretical calculations of Choi *et al* overestimate the differential cross sections at all angles by about 50% on average while the present results overestimate by about 30% on average. At 75 and 100 eV and for $\theta > 100°$, the present theory overestimates experimental results by about a factor of two. In figure 10, results at higher energies (200–800 eV) are compared with the absolute experimental values of Bromberg (1970) and Dubois and Rudd (1976). It is seen from figure 10 that the present calculations for e–CO are in very good agreement with experiment at all angles, except at some intermediate angles at 200 and 300 eV. In this energy region (200–800 eV), the cross sections of N_2 and

CO are almost equal, a fact which has been observed experimentally (Dubois and Rudd 1976).

Another assessment of the present results for CO at 400 and 500 eV is shown in figure 11, in which the ratio R

$$R = \frac{d\sigma/d\Omega}{I_C + I_O} \tag{15}$$

is plotted as a function of the scattering angle θ. For the experimental points (full and open circles in figure 11), R has been evaluated with the experimental values of Bromberg (1970) for $d\sigma/d\Omega$ and the theoretical values for each of the atomic DCS I_C and I_O (C and O stand for the carbon and oxygen atoms, respectively). Present theory reproduces all the maxima and minima almost at the same angle. Quantitatively, theory overestimates the ratio R by less than about 10% at all angles.

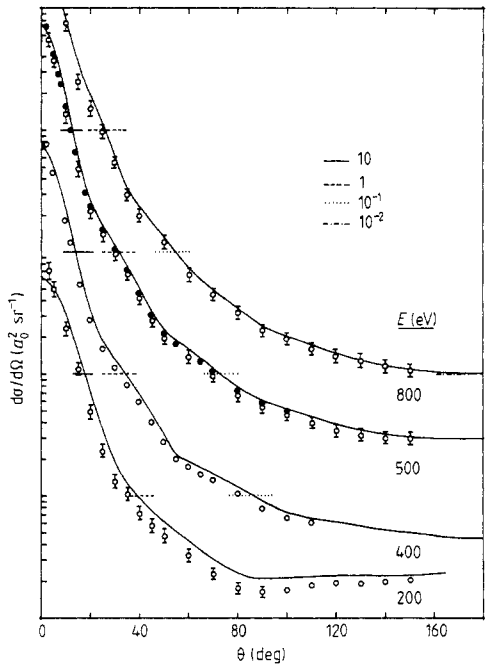

Figure 10. Same as in figure 4, but the full curves show the results of the present theory for e–CO.

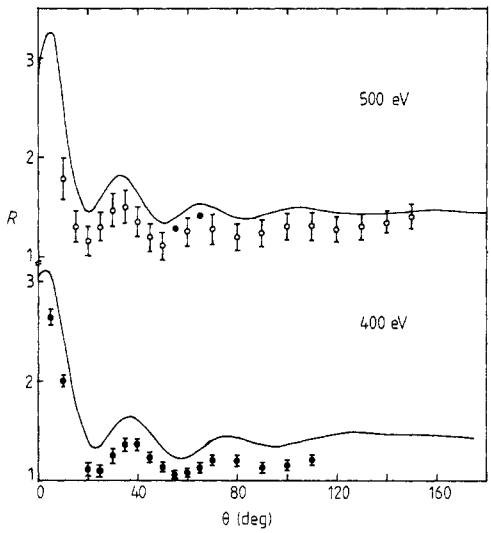

Figure 11. Ratio R (equation (15)) for e–CO collisions at 400 and 500 eV. Full curves, present calculations; ● and ○ are the experimental values due to Bromberg (1970) and Dubois and Rudd (1976), respectively.

In order to see further the quality of the present DCS, we also calculated the integral and the momentum transfer cross sections using equation (3). For N_2, these integral (σ_i) and momentum transfer (σ_m) cross sections are compared with experiment (Shyn and Carignan 1980, Dubois and Rudd 1976, Blaauw *et al* 1976, Jansen *et al* 1976) in figure 12. Also shown in figure 12 are the theoretical data (broken curves) of Choi *et al* (1979) for σ_i and σ_m. It is clear that the integral cross section compares well with experiment at all the energies considered here. However, the best agreement of the present integral cross section is with the latest measurements of Shyn and Carignan (1980). For σ_m, the overall agreement is good except at 100 eV where the discrepancy between the present theory and observation is about 25%. Figure 13 shows the present results for e–CO for σ_i and σ_m along with the observed

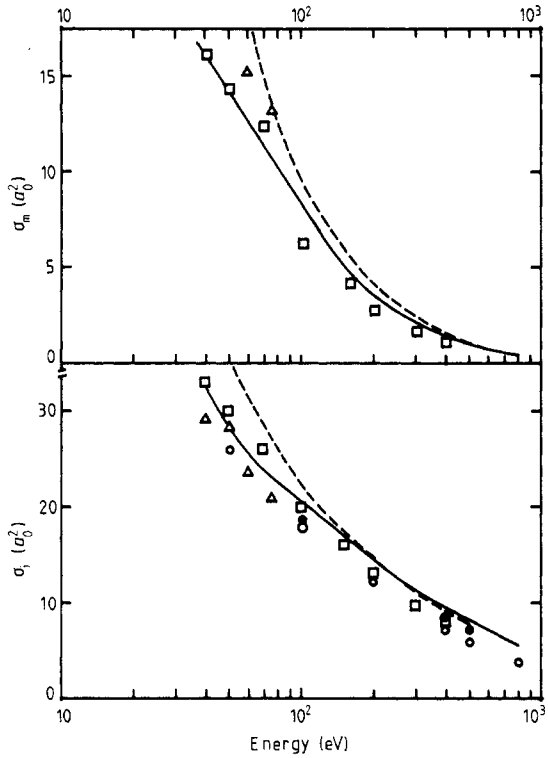

Figure 12. Integrated (σ_i) and momentum transfer (σ_m) cross sections for the e–N_2 scattering. Full curves, present theory. Experimental points are due to: △, Srivastava *et al* (1976); □, Shyn and Carignan (1980); ○, Dubois and Rudd (1976); ●, Jansen *et al* (1976); × Blaauw *et al* (1976).

data of Tanaka *et al* (1978) and Truhlar *et al* (1972b) and the theoretical values calculated by Choi *et al* (1979). Here, the present values overestimate the experiment by about a factor of 1.5 (the results of Choi *et al* are higher than the experiment by about a factor of three). On the other hand, σ_i and σ_m for N_2 compare quite well with recent absolute measurements (figure 12). It seems that the values for σ_i and σ_m of Tanaka *et al* are not accurate. They were calculated from the experimental differential cross section curves by extrapolating it from 15–0° and 130–180° and for this purpose they employed calculations of Choi *et al*. The experiments and theoretical calculations suggest that all cross sections for N_2 and CO at all energies (40–800 eV) do not differ very much from each other. However, the total cross sections of Tanaka *et al* for e–CO are not consistent with the corresponding values (experimental) for e–N_2. For example, at 50 eV, the value of σ_i for N_2 (28.6, Srivastava *et al* 1976) and for CO (19.7, Tanaka *et al* 1978) differ from each other by a factor of 1.45. In table 3, we give the cross sections (σ_i and σ_m) of N_2 and CO. It appears from this table that above 200 eV N_2 and CO have almost the same cross sections (σ_i and σ_m), but below 100 eV CO cross sections are higher than the N_2 ones by not more than 8%. Here, theory does not agree with experiment, where Dubois and Rudd (1976) have found that, except below 100 eV, N_2 cross sections may be larger than those of CO. In view of the fact that we neglected exchange and anisotropic shielded potentials, which may change the present predictions, more accurate calculations in the energy

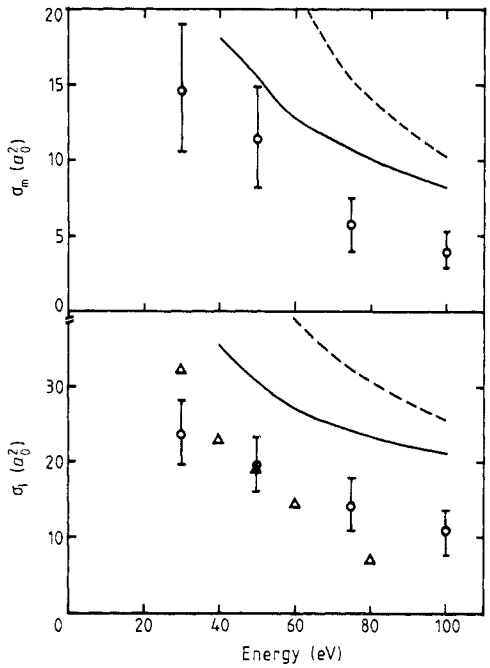

Figure 13. The cross sections σ_i and σ_m for e–CO scattering. Theory: full curves, present; broken curves, Choi *et al* (1979). Experiment: ○, Tanaka *et al* (1978); △, Truhlar *et al* (1972b).

Table 3. Total (σ_i) and momentum transfer (σ_m) cross sections (in a_0^2) for N_2 and CO.

	σ_i		σ_m	
Energy (eV)	N_2	CO	N_2	CO
40	32.79	35.61	16.26	18.39
50	28.47	30.81	14.37	15.74
60	25.71	27.20	12.77	12.72
75	23.13	24.43	10.80	10.74
100	20.38	21.43	8.25	8.22
200	14.40	14.51	3.61	3.59
400	9.51	9.49	1.39	1.37
500	8.17	8.14	0.99	0.98
800	5.81	5.78	0.48	0.47

region (40–100 eV) are required. However, the present theory is not able to give a definite answer to this discrepancy between N_2 and CO total cross sections at intermediate energies.

4. Conclusions

We have reported elastic cross sections for e–N_2 and e–CO at intermediate and high energies. From the results we draw the following conclusions.

(i) In any two-potential formalism (using the IAM model directly or indirectly) the second-order potential should be incorporated coherently.

(ii) Multiple scattering terms in the energy range 75–500 eV reduce the IAM cross section by up to about 25%.

(iii) Non-adiabatic effects in the polarisation potential, above 100 eV, should be taken into account either employing apparent polarisabilities or introducing an energy-dependent cut-off parameter.

(iv) Below 100 eV, the neglect of exchange and of the anisotropic part of the static potential causes a dip at intermediate angles that is deeper than the experimental one.

(v) Further, the present discrepancy in the theory and experiment, particularly at 100 and 200 eV, may be expected due to neglect of molecular binding (valence–core) effects. For H_2, the effect of molecular binding reduces the IAM cross sections by up to 30% (Jain *et al* 1979). For heavier systems such as CO and N_2, no simple way is known to incorporate such effects within the IAM. However, using anisotropic terms in the description of the present V_S potential would allow one indirectly to take an account of chemical bonds.

Acknowledgments

The author would like to thank Dr H R J Walters for many useful discussions. Part of the work was done at the University of Roorkee, India, where the author has benefitted from discussions with Drs M K Srivastava and A N Tripathi.

The author is greatly indebted to the staff of the Computer Centre (Queen's University) for the generous use of their machine. Financial support from the Queen's University, Belfast is gratefully acknowledged. He is particularly grateful to the referee for correcting some errors in the original manuscript and also to Dr D G Thompson for reading the revised manuscript.

References

Blaauw H J, Wagenaar R W, Barends D H and de Heer F J 1980 *J. Phys. B: At. Mol. Phys.* **13** 359–76
Bromberg J P 1970 *J. Chem. Phys.* **52** 1243–7
Bullard E C and Massey H S W 1931 *Proc. R. Soc.* A **133** 637
Choi B H, Poe R T and Sun J C 1979 *Phys. Rev.* A **19** 116–24
Chutjian A and Tanaka H 1980 *J. Phys. B: At. Mol. Phys.* **13** 1901–8
Cox H L Jr and Bonham R A 1967 *J. Chem. Phys.* **47** 2599–608
Dalba G, Fornasini P, Grisenti R, Ranieri G and Zecca A 1980 *J. Phys. B: At. Mol. Phys.* **13** 4695–701
Dubois R D and Rudd M E 1976 *J. Phys. B: At. Mol. Phys.* **9** 2657–67
Hayashi S and Kuchitsu K 1976a *J. Phys. Soc. Japan* **41** 1724–32
—— 1967b *Chem. Phys. Lett.* **41** 575–9
—— 1977 *J. Phys. Soc. Japan* **42** 1319–26
Herman D, Jost K and Kessler J 1976 *J. Chem. Phys.* **64** 1–5
Jain A, Tripathi A N and Srivastava M K 1979 *Phys. Rev.* A **20** 2352–5
Jansen R H J, de Heer F J, Luyken H J, Van Wingerden B and Blaauw H J 1976 *J. Phys. B: At. Mol. Phys.* **9** 185–212
Khare S P and Raj D 1979 *J. Phys. B: At. Mol. Phys.* **12** L351–4
Lane N F 1980 *Rev. Mod. Phys.* **52** 29–119
Lee Mu-Tao and Freitas L C G 1981 *J. Phys. B: At. Mol. Phys.* **14** 1053–64
Massey H S W 1935 *Trans. Faraday Soc.* **31** 556

Onda K and Truhlar D G 1979 *J. Chem. Phys.* **71** 5097–106
—— 1980 *J. Chem. Phys.* **73** 2688–95
Rumble J R and Truhlar D G 1979 *J. Chem. Phys.* **70** 4101–7
Sawada T, Ganas P S and Green A E 1974 *Phys. Rev.* A **9** 1130
Shyn T W and Carignan G R 1980 *Phys. Rev.* A **22** 923–9
Srivastava S K, Chutjian A and Trajmar S 1976 *J. Chem. Phys.* **64** 1340–4
Tanaka H, Srivastava S K and Chutjian A 1978 *J. Chem. Phys.* **69** 5329
Truhlar D G 1972 *Chem. Phys. Lett.* **15** 486–9
Truhlar D G, Onda K, Eades R A and Dixon D A 1979 *Int. J. Quant. Chem.* **13** 601, 632
Truhlar D G, Trajmar S and Williams W 1972a *J. Chem. Phys.* **57** 3250
Truhlar D G and Van-Catledge F A 1978 *J. Chem. Phys.* **69** 3575–8
Truhlar D G, Williams W and Trajmar S 1972b *J. Chem. Phys.* **57** 4307
Wedde T and Strand T G 1974 *J. Phys. B: At. Mol. Phys.* **7** 1091–100
Yates A C 1971 *Comput. Phys. Commun.* **2** 175–9
Yates A C and Temny A 1972 *Phys. Rev.* A **5** 2472–81